



**HAL**  
open science

## Phosphasalen vs. Salen Ligands: What Does the Phosphorus Change?

Irene Mustieles Marín, Audrey Auffrant

► **To cite this version:**

Irene Mustieles Marín, Audrey Auffrant. Phosphasalen vs. Salen Ligands: What Does the Phosphorus Change?. *European Journal of Inorganic Chemistry*, 2018, 2018 (15), pp.1634-1644. 10.1002/ejic.201701210 . hal-01999398

**HAL Id: hal-01999398**

**<https://hal.science/hal-01999398>**

Submitted on 22 Dec 2020

**HAL** is a multi-disciplinary open access archive for the deposit and dissemination of scientific research documents, whether they are published or not. The documents may come from teaching and research institutions in France or abroad, or from public or private research centers.

L'archive ouverte pluridisciplinaire **HAL**, est destinée au dépôt et à la diffusion de documents scientifiques de niveau recherche, publiés ou non, émanant des établissements d'enseignement et de recherche français ou étrangers, des laboratoires publics ou privés.

# Phosphasalen vs salen ligands: what does the phosphorus change?

Irene Mustieles Marín,<sup>[a]</sup> and Audrey Auffrant<sup>\*[a]</sup>

To the memory of Pr. P. Le Floch

**Abstract:** Phosphasalen ligands can be viewed as the phosphorous analogues of salen, in which the imine functions were replaced by iminophosphoranes (P=N). Their divergent stereo-electronic properties compared to salen, i. e., larger electron-donation, higher flexibility, and larger steric hindrance due to the presence of two substituents on the tetrahedral phosphorus atoms, were exploited in coordination chemistry and catalysis. They were proved to be able to stabilize metals in unusual oxidation states; square planar copper(III) and nickel(III) complexes were isolated. Because of the redox non-innocent character of these ligands, the electronic structure of the one-electron oxidized complexes was studied in depth to determine the metallic vs ligand contribution in the overall delocalization. In addition, the catalytic activity of different phosphasalen complexes was proved in ring opening polymerization of lactide, and rare-earth phosphasalen complexes were shown to be powerful, rapid, controlled, and stereoselective initiators. Importantly, the stereochemical outcome of the reaction can be tuned by changing the ligand structure or the metal. In particular, efficient iso-selective initiators were developed.

## 1. Introduction

N,N-bis(salicylidine)ethylenediamines, generally called in short "salen", are a family of very successful ligands in coordination chemistry.<sup>[1]</sup> Their applications encompass catalysis,<sup>[2]</sup> bio-inorganic chemistry,<sup>[3]</sup> as well as material science.<sup>[3b, 4]</sup> Their popularity stems from their easy synthesis allowing facile structural variations and their ability to coordinate a wide range of metals in various oxidation states. However, among all the skeleton variations proposed, only few concern the introduction of a heteroatom in place of the carbon in the imine function, with the exception of some azo derivatives.<sup>[5]</sup>

The introduction of phosphorus gave phosphasalen ligands, as we termed them, in which the imine groups have been substituted by iminophosphorane (P=N) functions (see Figure 1). First complexes of this family were reported in 2011. The group of P. Diaconescu described the coordination of a phosphasalen type ligand incorporating a ferrocene unit (labeled as Psalfen thereafter), to cerium and yttrium centers (see Figure 2).<sup>[6]</sup> Our group reported the synthesis and characterization of group 10 phosphasalen complexes.<sup>[7]</sup>

The presence of the iminophosphorane functions in the salen

backbone induces both electronic and geometric changes. Regarding the electronic properties, the most important difference is the absence of a  $\pi$ -system. In the iminophosphorane function the nitrogen atom possesses two lone pairs which are stabilized by delocalization in the  $\sigma$ -anti-bonding orbitals of the P-C bonds.<sup>[8]</sup> This so-called negative hyperconjugation induces a strong interaction between the phosphorus and the nitrogen atoms which is commonly pictured by a double bond. However, iminophosphorane functions can be better described as masked amides.

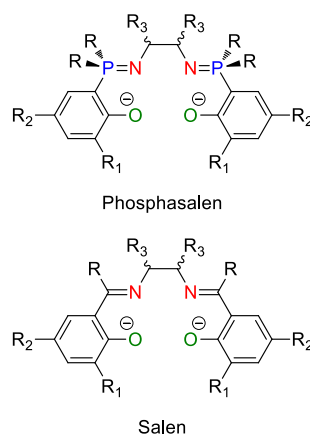


Figure 1: Salen and Phosphasalen general structure

Thus, they are strong  $\sigma$ - and  $\pi$ -donors with almost no accepting ability, while imine functions are  $\sigma$ -donating and  $\pi$ -accepting. Interestingly, the electron-donating properties of the iminophosphorane functions can be tuned via the nitrogen and phosphorus substituents. Those featuring an aryl group on the nitrogen atom are less electron-donating than those bearing an alkyl because of a partial delocalization of the nitrogen lone pairs on the aromatic ring. The substituents on the phosphorus atom influence its ability to stabilize the lone pairs of the nitrogen atoms. The negative hyperconjugation increases when the phosphorus bears aromatic substituents. The donation of the iminophosphorane is therefore enhanced by the presence of alkyl substituents on P or N atoms. Regarding the geometry, iminophosphoranes are not planar as the  $sp^2$  hybridized imines since the phosphorus atom is engaged in four bonds. Indeed, the phosphorus bears two substituents while there is only one on the carbon of the imine. In addition, the bond lengths are not comparable (PN  $\sim$  1.58 Å vs CN  $\sim$  1.28 Å)

Therefore, phosphasalen complexes differ markedly from their carbon analogues. The purpose of this microreview is to give an overview of the recent results obtained with this new type of phosphorus based ligands. It will be shown how the presence of

[a] Dr. I. Mustieles Marín and Dr. A. Auffrant  
LCM  
CNRS-Ecole polytechnique, Université Paris-Saclay,  
F-91128 Palaiseau Cedex  
E-mail: [audrey.auffrant@polytechnique.edu](mailto:audrey.auffrant@polytechnique.edu)

the heteroatom can influence the geometry, the electronic structure, as well as the catalytic ability, compared to salen analogues.

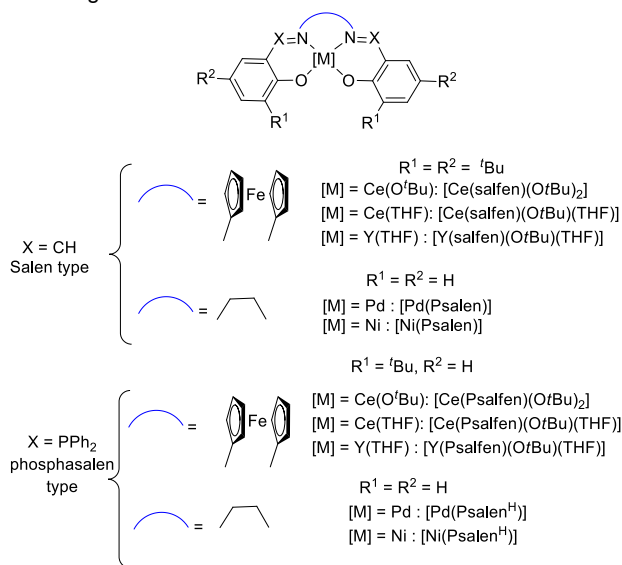
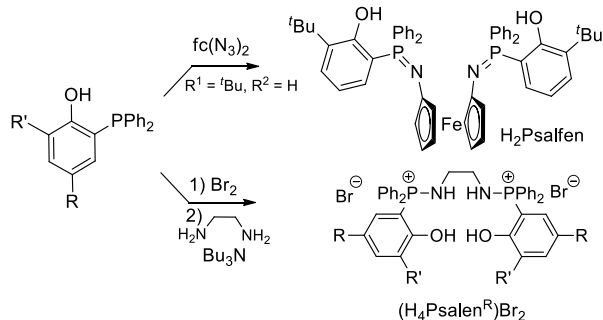


**Figure 2.** Structure of the first phosphasalens complexes and their salen analogues.

## 2. Synthesis, structure and electronic properties of phosphasalens complexes

### 2.1. Ligand synthesis, coordination and solid state structure

The structures of the first phosphasalens complexes are presented in Figure 2 together with that of their salen counterparts.



**Scheme 1.** Phosphasalens ligand synthesis.

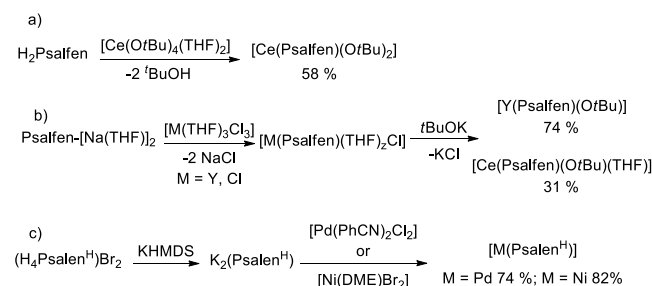
The synthesis of the phosphasalens platform starts from *o*-phosphinophenol. The introduction of the iminophosphorane function can then be achieved by two main strategies: the Staudinger reaction,<sup>[9]</sup> consisting in the condensation of a phosphine and an azide, or the modified Kirsanov reaction,<sup>[10]</sup> involving the halogenation of a phosphine followed by the

trapping of the intermediate by a primary amine in presence of a sacrificial base.

The group of Diaconescu<sup>[6]</sup> relied on the first synthetic method to prepare the neutral H<sub>2</sub>Psalfen proligand (Scheme 1, top) because of the availability of 1,1'-diazidoferrocene. They were, by this way, able to isolate and coordinate the phosphazide intermediate (P=N-N=N) derivative.

We preferred to rely on a modified Kirsanov reaction<sup>[7]</sup> allowing the use of diamines, thus avoiding the employ of potentially explosive azido compounds (Scheme 1, bottom). So, we isolated the corresponding bis(aminophosphonium) salts which are rather stable and can be stored almost indefinitely on the bench without any specific precautions. On the contrary, iminophosphorane derivatives are sensitive to moisture.

Coordination reactions can be performed by mixing the neutral proligand with a metal precursor featuring basic ancillary ligands, as done for the Ce<sup>IV</sup> complex via the reaction between H<sub>2</sub>Psalfen and [Ce(OtBu)<sub>4</sub>(THF)<sub>2</sub>] (Scheme 2a). It is also possible to generate the dianionic ligand, using sodium or potassium hexamethyldisilazane or hydride, and make it react with the metal chloride precursor as done for Ce<sup>III</sup>, Y<sup>III</sup>, Pd<sup>II</sup>, and Ni<sup>II</sup> complexes (see Scheme 2b and c). In these syntheses, the anionic ligands were not isolated because of their sensitivity, but this was done in some other cases (vide section 4). The synthesis of rare-earth complexes was completed by metathesis with tBuOK. All diamagnetic complexes were characterized by multinuclear NMR spectroscopy. Coordination is evidenced by a deshielding of the <sup>31</sup>P nuclei compared to the corresponding proligands: δ<sub>P</sub> = 34.6, 32.6, 33.7, and 32.8 ppm for [Ce(Psalfen)(OtBu)(THF)], [Y(Psalfen)(OtBu)], [Pd(Psalen<sup>H</sup>)], and [Ni(Psalen<sup>H</sup>)] respectively, to compare with 27.1 ppm for H<sub>2</sub>Psalfen and 18.6 ppm for K<sub>2</sub>Psalfen<sup>H</sup>.



**Scheme 2.** Formation of phosphasalens complexes.

The characterization of [Ce(Psalfen)(OtBu)<sub>2</sub>], [Pd(Psalen<sup>H</sup>)], and [Ni(Psalen<sup>H</sup>)] by X-ray diffraction analysis allows discussing the geometrical modifications compared to the structures of the salen analogues. For these three complexes, the M-O and M-N distances measured are larger than in the corresponding salen complexes. The deviation from planarity also increases with the introduction of the phosphorus. In the cerium complex, the NCeOC<sub>0</sub> torsion angle (see Figure 3 for labeling) was measured at about 45 ° in the Psalfen complex<sup>[6]</sup> vs 4.5 ° in the salen analogue. A larger distortion was also observed in [Pd(Psalen<sup>H</sup>)] and [Ni(Psalen<sup>H</sup>)]<sup>[7]</sup> compared to their salen counterpart:<sup>[11]</sup> the NMOC<sub>0</sub> torsion angle was measured at 25.64 and 22.57 ° in

[Pd(Psalen<sup>H</sup>)] and [Ni(Psalen<sup>H</sup>)] respectively, while these are at 3.02 and 3.30 ° in the corresponding salen derivatives. This evidences the bending of the phenoxide rings relative to the main coordination plane. These geometrical differences arise from the tetrahedral arrangement of the phosphorus bearing one additional substituent compared to the imine carbon and the difference in bond lengths between C=N and P-N. These differences make phosphasalens more flexible than salen ones.

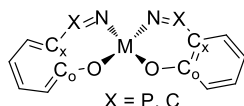


Figure 3. Labeling for geometrical considerations.

## 2.2. Influence of iminophosphorane on electronic and magnetic properties

Phosphasalens ligands also differ a lot in terms of electronics as show by cyclic voltammetry experiments.

Table 1. Redox events for phosphasalens<sup>[6-7]</sup> and salen<sup>[12]</sup> complexes.

Entry	Complex	Reduction <sup>a</sup>	Oxidation <sup>a</sup> E <sub>1/2</sub> <sup>ox1</sup>
1	[Y(Psalen)(OtBu)] <sup>b,c</sup>		-0.29
2	[Y(salphen)(OtBu)(THF)] <sup>b,d</sup>		0.09
3	[Ce(Psalen)(OtBu)(THF)] <sup>b,c</sup>		-0.57
4	[Ce(salphen)(OtBu)(THF)] <sup>b,d</sup>		-0.21 <sup>i</sup> ; -1.05 <sup>k</sup>
5	[Ce(Psalen)(OtBu) <sub>2</sub> ] <sup>b,c</sup>	-1.70 <sup>i</sup> ; -2.07 <sup>k</sup>	-0.38
6	[Ce(salphen)(OtBu) <sub>2</sub> ] <sup>b,d</sup>	-1.01 <sup>i</sup> ; -2.39 <sup>k</sup>	-0.28
7	[Pd(Psalen <sup>H</sup> )] <sup>e,f</sup>		0.27
8	[Pd(salen <sup>H</sup> )] <sup>g</sup>		0.44; 0.55
9	[Ni(Psalen <sup>H</sup> )] <sup>e,h</sup>		0.1
10	[Ni(salen <sup>H</sup> )] <sup>i</sup>		0.33

<sup>a</sup> Potentials expressed in V versus Fc<sup>+</sup>/Fc. <sup>b</sup> in THF, with 0.5 mol L<sup>-1</sup> [nPr<sub>4</sub>][BAF<sub>4</sub>]; scan rate = 250 mV s<sup>-1</sup>. <sup>c</sup> c = 1.5 mmol L<sup>-1</sup>. <sup>d</sup> c = 2.0 mmol L<sup>-1</sup>. <sup>e</sup> in DMF/CH<sub>3</sub>CN 60/40, with 0.12 mol L<sup>-1</sup> NBu<sub>4</sub>BF<sub>4</sub>; scan rate = 100 mV s<sup>-1</sup>. <sup>f</sup> c = 2.0 mmol L<sup>-1</sup>. <sup>g</sup> c = 1 mmol L<sup>-1</sup> in CH<sub>3</sub>CN with 0.1 mol L<sup>-1</sup> NBu<sub>4</sub>ClO<sub>4</sub> see ref. [12b]. <sup>h</sup> c = 3.8 mmol L<sup>-1</sup>. <sup>i</sup> c = 1 mmol L<sup>-1</sup> in CH<sub>3</sub>CN with 0.1 mol L<sup>-1</sup> NEt<sub>4</sub>ClO<sub>4</sub> see ref. [12a]. <sup>j</sup> anodic potential. <sup>k</sup> cathodic potential.

Data of yttrium, cerium, palladium and nickel phosphasalens complexes, and those of their salen analogues are gathered in Table 1. All potentials given are relative to Fc<sup>+</sup>/Fc for sake of comparison.

The oxidation turns out to be easier for phosphasalens complexes than for salen ones. Indeed, the potential measured

for the oxidation of the ferrocene unit in yttrium(III) and cerium(IV) Psalens complexes is lowered by 0.38 and 0.10 V compared to salen ones (Table 1, entries 1 and 5 vs 2 and 6).<sup>[6]</sup> In palladium and nickel Psalens<sup>H</sup> complexes, the oxidation is lowered by about 0.2 V when introducing the iminophosphoranes (Table 1, entries 7-10).<sup>[7]</sup> Reduction was only observed with the cerium(IV) complexes (Ce<sup>IV</sup>/Ce<sup>III</sup>), and is more difficult in presence of the Psalens ligand than with the salen one.<sup>[6]</sup> The better electron-donating ability of iminophosphoranes is responsible for the observed shifts in the redox potentials.

The presence of the phosphorus also influences the magnetic properties. [Ni(Psalen<sup>H</sup>)] complex presents a low magnetic moment in solution, measured at 1.4 μ<sub>B</sub> at room temperature by the Evans method whereas [Ni(salen<sup>H</sup>)] did not, suggesting a low lying triplet state. To understand the origin of this behavior, which contrasts with the diamagnetism of [Ni(salen<sup>H</sup>)], DFT calculations were performed. They confirmed the small singlet-triplet energy difference and demonstrated that the easier ionization of the Psalens<sup>H</sup> complex is responsible for the lowering of the singlet-triplet energy gap.<sup>[7]</sup>

## 3. One-electron oxidation of phosphasalens nickel and copper complexes

The oxidation of salen complexes was largely studied in order to bring a better understanding of reaction mechanisms in homogeneous catalysis or at the active site of metalloenzymes. Indeed, their N<sub>2</sub>O<sub>2</sub> coordination sphere can in some cases be mimicked by the salen platform. From a fundamental perspective, the determination of the electronic structure of one-electron oxidized salen complexes is challenging because of the redox-non innocence of the ligand. The oxidation can take place either on the ligand, leading to a phenoxyl radical or on the metal. As galactose oxidase (GO) was proved to incorporate in its active site a copper(II) center and a tyrosyl radical, the electronic structure of mono-oxidized copper(II) salen complexes was much investigated. They were generally characterized as a Cu<sup>II</sup>-ligand radical complex (Cu<sup>III</sup> was evidenced in only two cases).<sup>[3a, 13]</sup> Nickel complexes received also much attention, which may be explained by the vicinity of both metals in the periodic table and the involvement of Ni-based metalloenzyme, such as superoxide dismutase (SOD), in enzymatic oxidation reactions.<sup>[14]</sup> In that case, the catalytic relevant species was characterized as a Ni<sup>III</sup> complex. Salen proved capable to stabilize a high-valent Ni<sup>III</sup> center in an octahedral environment,<sup>[15]</sup> while mono-oxidation leads to nickel(II) phenoxyl radical complexes in absence of exogenous ligands.<sup>[16]</sup> Because of the geometric and electronic differences due to the presence of the phosphorus atom, the electronic structures of one-electron oxidized phosphasalens complexes merits further study. As the iminophosphorane function can be viewed as a phosphonium-nitrogen ylide (P<sup>+</sup>-N<sup>-</sup>), its incorporation within the ligand backbone should decrease the electron density on the phenolates (because of the presence of an electropositive phosphorus atom) as well as increase the electron donation

from the nitrogen atoms. The phosphasalen platform should therefore favor a metal-centered oxidation (compared to salen) and may be able to stabilize the high-valent metal in a tetra-coordinated environment. Copper and nickel complexes were investigated because of the precedent studies on salen derivatives and the recent interest for the synthesis and characterization of high-valent copper(III)<sup>[17]</sup> and nickel(III/IV) complexes. Examples of Ni<sup>IV</sup> complexes remain scarce,<sup>[18]</sup> while the Ni<sup>III</sup>/Ni<sup>IV</sup> redox couple<sup>[19]</sup> has started to be considered as an alternative to the Pd<sup>II</sup>/Pd<sup>IV</sup> couple in bond forming reactions. Ni<sup>III</sup> complexes have also recently found applications in synthesis,<sup>[20]</sup> and Cu<sup>III</sup> have been established as key intermediates in various catalytic reactions.<sup>[21]</sup> Most importantly, the precise determination of the electronic structure of a complex can be very complicated in presence of redox non-innocent ligands<sup>[22]</sup> such as those containing phenoxide units. Depending on the nature of the redox-active orbitals in such complexes, the redox processes can take place either on the metal or on the ligand. Therefore, different electronic configurations are possible for nickel and copper complexes. In the former, the oxidation leads to a paramagnetic complex which can be either a high-valent d<sup>7</sup> Ni<sup>III</sup> complex or a ligand radical complex (Figure 4).

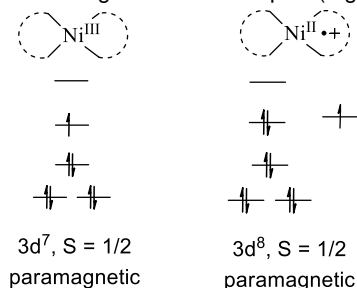


**Figure 4.** Representation of the possible electronic configurations for one-electron oxidized nickel complexes in a square planar environment.

In the case of copper, the oxidation can give a diamagnetic Cu<sup>III</sup> complex (closed-shell singlet configuration), if the oxidation takes place on the metal. If the electron is removed from the ligand, the resulting d<sup>9</sup> complex can be either diamagnetic, if the unpaired electron on the metal and the one on the ligand couple antiferromagnetically (open-shell singlet configuration), or paramagnetic if they couple ferromagnetically leading to a triplet (Figure 5).

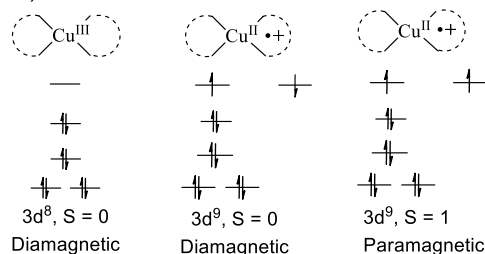


**Figure 5.** Representation of the possible electronic configuration for one-electron oxidized copper complexes in a square planar environment.

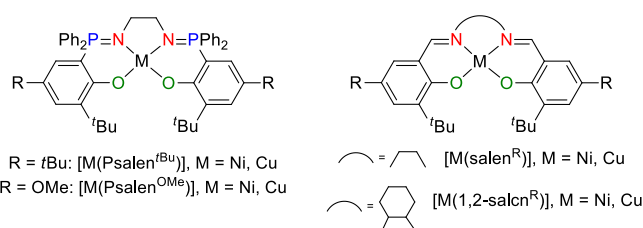


**Figure 6.** Structure of Psalen<sup>tBu</sup> and Psalen<sup>OMe</sup> complexes and their salen analogues.

Figure 6 shows the structure of the four phosphasalen complexes investigated and their salen precedents (Figure 6).

For this study a ligand featuring *ortho* and *para*-substituted phenoxide rings was employed, *tert*-butyl substituents were chosen for solubility reason (Psalen<sup>tBu</sup>).<sup>[23]</sup> In order to determine the influence of the phenoxide substituents, the Psalen<sup>OMe</sup> ligand, where the *para* position on each phenoxide ring is occupied by a methoxy group, was also employed.<sup>[24]</sup>

The electronic structure of the corresponding salen complexes was investigated: [Ni(salen<sup>tBu</sup>)]<sup>+</sup> was described as a delocalized radical complex in the absence of exogenous ligands,<sup>[15c, 25]</sup> while the introduction of a methoxy group ([Ni(1,2-salcn<sup>OMe</sup>)]<sup>+</sup>) favors the formation of a localized phenoxy radical complex.<sup>[13b]</sup> The same structure was established for [Cu(1,2-salcn<sup>OMe</sup>)]<sup>+</sup>,<sup>[13b]</sup> whereas [Cu(1,2-salcn<sup>tBu</sup>)]<sup>+</sup> was described as a Cu<sup>III</sup> complex in the solid state. In solution, a spin equilibrium between the high-valent and the ligand radical species was suggested.

The phosphasalen ligands and complexes shown in Figure 6 were synthesized following the described methodology (see Schemes 1 and 2), and their electronic properties were investigated by cyclic voltammetry. Nickel phosphasalen complexes exhibit three oxidation waves: a first reversible, a second pseudo-reversible and a last one irreversible, which accounts for the possibility to oxidize the metal and the two phenoxide rings. The copper complexes display two reversible oxidations, which can correspond to the sequential oxidation of both phenoxide rings or that of the metal and one phenoxide. Table 2 gathers oxidation potential values for the phosphasalen complexes and their carbon analogues. As already noticed, oxidations are easier for phosphasalen complexes than salen ones. In the case of the nickel derivatives, the better electron-donating ability of Psalen ligands allows the observation of three oxidations, while in salen complexes, only two oxidation waves are observed. Moreover, oxidations are further facilitated by the electron-rich methoxy groups in the same extent for nickel and copper complexes ( $\Delta E = 0.07$  and  $0.06$  V). The gap between the first and the second oxidation ( $\Delta E_{1-2}$ ) was used as an indication of the delocalization within the one-electron oxidized complex, translating how the first oxidation influences the second one.<sup>[15c]</sup> A large value in the case of [Ni(salen<sup>tBu</sup>)] (0.46 V) was ascribed to a strong electrochemical communication. This gap was measured at 0.81 and 0.53 V for [Ni(Psalen<sup>tBu</sup>)] and [Ni(Psalen<sup>OMe</sup>)], at 0.85 and 0.50 V for [Cu(Psalen<sup>tBu</sup>)] and [Cu(Psalen<sup>OMe</sup>)] respectively. These comparable  $\Delta E_{1-2}$  values for nickel and copper complexes when featuring the same ligand suggest similar electronic structure of the mono-oxidized species.

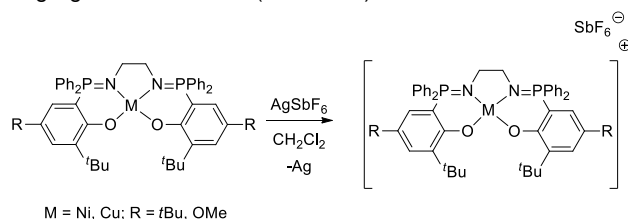
The gaps observed for phosphasalens complexes are much larger than those reported for the corresponding salen derivatives suggesting that the metal is more and more affected by the first oxidation on going from salen<sup>tBu</sup>, Psalen<sup>OMe</sup> to Psalen<sup>tBu</sup> ligands.

**Table 2.** Redox potentials for Psalen and salen nickel and copper complexes.<sup>a</sup>

Compound	E <sup>1/2</sup>	E <sup>2/2</sup>	ΔE <sub>1-2</sub>	E <sub>a</sub> <sup>3</sup>	ΔE <sub>2-3</sub>
[Ni(Psalen <sup>tBu</sup> )] <sup>b</sup>	0.001	0.82	0.81	1.07	0.26
[Ni(Psalen <sup>OMe</sup> )] <sup>b</sup>	-0.06	0.47	0.53	1.00	0.53
[Ni(salen <sup>tBu</sup> )] <sup>c,d</sup>	0.59	1.05	0.46	-	-
[Ni(1,2-salcn <sup>OMe</sup> )] <sup>c,e</sup>	0.22	0.64	0.42	-	-
[Cu(Psalen <sup>tBu</sup> )] <sup>b</sup>	0.10	0.95	0.85	-	-
[Cu(Psalen <sup>OMe</sup> )] <sup>b</sup>	0.04	0.54	0.50	-	-
[Cu(salen <sup>tBu</sup> )] <sup>c,f</sup>	0.55	0.75	0.20	-	-
[Cu(1,2-salcn <sup>OMe</sup> )] <sup>c,e</sup>	0.28	0.44	0.16	-	-

<sup>a</sup> measured in CH<sub>2</sub>Cl<sub>2</sub> and expressed in V versus Fc<sup>+/0</sup>. <sup>b</sup> c = 3 mmol L<sup>-1</sup> for the complex, 0.12 mol L<sup>-1</sup> NBu<sub>4</sub>PF<sub>6</sub>, see ref. [24]; <sup>c</sup> c = 1 mmol L<sup>-1</sup> for the complex, 0.1 mol L<sup>-1</sup> NBu<sub>4</sub>PF<sub>6</sub>. <sup>d</sup> ref. [15c]. <sup>e</sup> ref. [13b]. <sup>f</sup> ref. [26].

To investigate the electronic structure of the cationic phosphasalens complexes,<sup>[20b]</sup> they were synthesized in high yield using Ag<sup>I</sup> salts as oxidant (Scheme 3).



**Scheme 3.** Oxidation of phosphasalens complexes.

Their structure was studied employing various spectroscopic techniques and quantum chemical calculations. X-ray structures of cationic nickel complexes showed a contraction of the coordination sphere, which is not identical for all atoms so that a long NNiO axis appears upon oxidation. The oxidation is accompanied by an amplification of the distortion relative to an ideal square planar geometry. Meanwhile, the phenoxy units do not experience much change; no quinoid pattern was observed. All these data therefore point towards the formation of high-valent Ni<sup>III</sup> complexes. In addition, the solid state magnetic measurements gave slightly different g<sub>iso</sub> values: 2.22 for [Ni(Psalen<sup>tBu</sup>)](SbF<sub>6</sub>) and 2.16 for [Ni(Psalen<sup>OMe</sup>)](SbF<sub>6</sub>). In agreement with X-ray data, these g values indicate a substantial

metallic character of the magnetic orbital. Nevertheless, the slightly decreased g value for [Ni(Psalen<sup>OMe</sup>)](SbF<sub>6</sub>) can be the sign of a lower metal character as suggested by the CV measurements. In solution, no <sup>31</sup>P resonance was observed for both complexes while their <sup>1</sup>H NMR spectra are typical of paramagnetic complexes, reinforcing the picture of d<sup>7</sup> complexes. However, subtle differences appear when considering their chemical shifts and in particular the isotropic paramagnetic shift (δ<sub>para</sub> = δ<sub>obs</sub> - δ<sub>dia</sub>). The isotropic shifts are larger for [Ni(Psalen<sup>OMe</sup>)](SbF<sub>6</sub>) than for [Ni(Psalen<sup>tBu</sup>)](SbF<sub>6</sub>). This was proposed to be related to a larger spin density on the phenoxy ring in [Ni(Psalen<sup>OMe</sup>)](SbF<sub>6</sub>).

The cationic phosphasalens complexes were also characterized by EPR spectroscopy since Mono-oxidized nickel(II) complexes have a doublet multiplicity. An unresolved signal centered at g = 2.034 was observed for [Ni(salen<sup>tBu</sup>)]<sup>+</sup> at 200 K,<sup>[15c]</sup> while [Ni(1,2-salcn<sup>OMe</sup>)]<sup>+</sup> gave a rhombic signal with g values of 2.015, 1.992, and 2.054 (g<sub>av</sub> = 2.02) at 100 K.<sup>[13b]</sup>

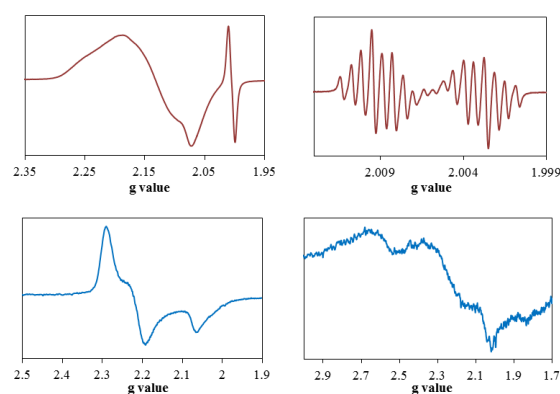


**Figure 7.** EPR spectra of [Ni(Psalen<sup>OMe</sup>)](SbF<sub>6</sub>) (top: left at 10K, right at 290 K) and [Ni(Psalen<sup>tBu</sup>)](SbF<sub>6</sub>) (bottom: left at 5 K, right at 252 K) in CH<sub>2</sub>Cl<sub>2</sub> solution.

[Ni(Psalen<sup>tBu</sup>)](SbF<sub>6</sub>) and [Ni(Psalen<sup>OMe</sup>)](SbF<sub>6</sub>) present different EPR spectra. At 290 K, [Ni(Psalen<sup>OMe</sup>)](SbF<sub>6</sub>) exhibits an isotropic complicated pattern centered at g<sub>iso</sub> = 2.005 corresponding to an organic radical (Figure 7, top right). When decreasing the temperature, the spectrum broadens, and below 100 K a new rhombic signal appears (g<sub>1</sub> = 2.22, g<sub>2</sub> = 2.14, and g<sub>3</sub> = 2.07, g<sub>av</sub> = 2.14, Figure 7, top left). It corresponds to a Ni<sup>III</sup> d<sup>7</sup> center in rhombic environment. A rhombic S = 1/2 signal was also observed for [Ni(Psalen<sup>tBu</sup>)](SbF<sub>6</sub>) at 5 K. For this complex, the signal broadens when increasing the temperature (see Figure 7, bottom right) without showing any other feature. For both complexes however, the solid state EPR spectrum agrees with a Ni<sup>III</sup> structure and no ligand signal was seen. The observation of both features (metallic and radical) in the EPR spectrum of [Ni(Psalen<sup>OMe</sup>)](SbF<sub>6</sub>) (Figure 7, bottom right) is not usual in these systems and can be explained by a strongly delocalized orbital, or a multi-configurational ground state with several configurations having either metallic or ligand character,

or by an incomplete valence tautomerism.<sup>[13c, 15c, d, 16e]</sup> It is very difficult to distinguish between these two last hypotheses. Nevertheless, a value of 1.9  $\mu_B$ , exceeding the spin-only value, was obtained as the effective magnetic moment of this complex in solution. This may indicate an orbital contribution to this moment and seems to tip the balance in favor of the multi-configuration rather than the valence tautomerism hypothesis.

For copper complexes, X-ray diffraction shows a contraction of the coordination sphere upon oxidation. This contraction is larger for  $[\text{Cu}(\text{Psalen}^{\text{Bu}})](\text{SbF}_6)$  than for  $[\text{Cu}(\text{Psalen}^{\text{OMe}})](\text{SbF}_6)$  which may be the sign of a different electronic structure. This contraction, together with the absence of significant variation in the metrics of the phenoxide, suggests in both case a metal-centred oxidation. Accordingly, these complexes are EPR silent between 77 and 293 K. However, EPR spectroscopy was poorly informative even for  $[\text{Cu}(1,2\text{-salcn}^{\text{OMe}})]^+$  and  $[\text{Cu}(\text{salen}^{\text{Bu}})]^+$ , for which oxidation occurs on the phenoxide. Their silent EPR spectra were explained by the nature of the coupling between the spin of the radical species and that of the  $\text{Cu}^{\text{II}}$  center.<sup>[13b, 26]</sup>

Nevertheless, the magnetic data for the cationic phosphasalen copper complexes do not fit with a pure  $d^8$  configuration as they both present a temperature independent paramagnetism (TIP). This corresponds to a singlet ground state and a high energy triplet state, which is almost not populated at room temperature (gap beyond  $1000\text{ cm}^{-1}$ ). Noteworthy, the  $\chi$  value measured on  $[\text{Cu}(\text{Psalen}^{\text{Bu}})](\text{SbF}_6)$  crystals was much lower than that of  $[\text{Cu}(\text{Psalen}^{\text{OMe}})](\text{SbF}_6)$  ( $0.0001(1)$  vs  $0.00070(5)\text{ cm}^3\text{ mol}^{-1}$ ), suggesting again some differences in the electronic structure of the two complexes. This was further evidenced by NMR studies. While  $[\text{Cu}(\text{Psalen}^{\text{Bu}})](\text{SbF}_6)$  displays a diamagnetic behavior:  $^{31}\text{P}$  and  $^1\text{H}$  NMR signals were observed at room temperature with almost no variation with the temperature,  $[\text{Cu}(\text{Psalen}^{\text{OMe}})](\text{SbF}_6)$  presents no  $^{31}\text{P}$  signal at room temperature and a broader  $^1\text{H}$  NMR spectrum with some resonances being particularly shifted. The variable temperature NMR study evidenced a nonlinear evolution of the chemical shifts, which fitting allowed the determination of various parameters. The energy gap between the singlet and triplet state evaluated at  $1420\text{ cm}^{-1}$  ( $\sim 17\text{ kJ mol}^{-1}$ ) is in agreement with that anticipated by magnetic measurements. The chemical shifts corresponding to the singlet state were also obtained; they slightly differ from those observed at  $-90\text{ }^\circ\text{C}$ .

DFT calculations were unable to give further indications about the electronic structure, since the computed HOMOs are very similar for all the oxidized complexes. CASSCF calculations were conducted pointing in each case to multi-configurational ground states in agreement with the experimental observations. This means that several configurations are necessary to accurately depict the ground state. It happens in a transition metal complex when, despite a decreased orbital overlap, the ligand and the metal remain close in energy so that bonding electrons can be located in different orbitals.<sup>[22b, d, e, 27]</sup> Very interestingly, the differences found depending on the ligands were well reproduced by these calculations. Thus, the main configuration obtained for  $[\text{Ni}(\text{Psalen}^{\text{Bu}})]^+$  corresponds to a single electron in a metal based orbital. For  $[\text{Ni}(\text{Psalen}^{\text{OMe}})]^+$ , the single electron is mainly localized in metal-ligand orbital with a

strong contribution of the phenoxide orbitals. For  $[\text{Cu}(\text{Psalen}^{\text{Bu}})]^+$ , the major configuration corresponds to a closed-shell singlet, while this configuration is minor in  $[\text{Cu}(\text{Psalen}^{\text{OMe}})]^+$ , for which the open-shell singlet was calculated to be major. This larger ligand character found experimentally and confirmed by the calculations can be ascribed to an increased electron density on the phenoxide rings when substituted by a methoxy group. Nevertheless, aside electronic factors the different coordination geometry offered by the phosphasalen platform may explain the differences observed with respect to salen derivatives. A better orbital mixing may be possible in phosphasalen compared to salen, and even more for the  $\text{Psalen}^{\text{OMe}}$  ligand than the  $\text{Psalen}^{\text{Bu}}$  one.

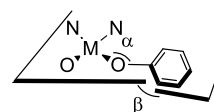


**Figure 8.** Definition of  $\alpha$  and  $\beta$  angles.

For the  $\text{Psalen}^{\text{Bu}}$  and  $\text{Psalen}^{\text{OMe}}$  nickel and copper complexes, the  $\alpha$  and  $\beta$  angles (see Figure 8) range from  $125$  to  $130\text{ }^\circ$  and  $32$  and  $44\text{ }^\circ$  respectively. These values are comparable with those of galactose oxidase,  $\alpha = 129\text{ }^\circ$  and  $\beta = 75\text{ }^\circ$  but differ much from those measured for salen complexes ( $180\text{ }^\circ$  and  $90\text{ }^\circ$ ). Thus, in phosphasalen complexes the orbital overlap increases resulting in a delocalized bonding orbital with both metal and ligand character. Moreover, a slight difference in the  $\beta$  angle was found in  $\text{Psalen}^{\text{OMe}}$  ( $44\text{ }^\circ$  on average) compared to  $\text{Psalen}^{\text{Bu}}$  ligand ( $36\text{ }^\circ$  on average) which may be at the origin of the larger ligand radical character evidenced in  $[\text{M}(\text{Psalen}^{\text{OMe}})]^+$  complexes. This geometrical factor may also play a role in the differences observed experimentally between solution and solid state measurements.

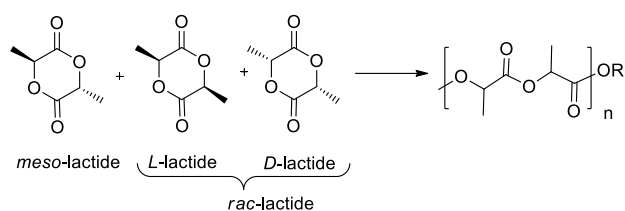
As this investigation of four mono-oxidized phosphasalen complexes points towards a multi-configurational ground state, in which the configuration corresponding to an oxidized metal is preponderant, further oxidations are assumed to be centered on the phenoxide rings. Nevertheless the precise electronic structure of  $[\text{M}(\text{Psalen})]^{2+}$  or even  $[\text{Ni}(\text{Psalen})]^{3+}$  would require a complete spectro-electrochemical study.

Moreover, the influence of other parameters such as nature of the N,N linker, as for salen ligands, but also that of the phosphorus substituents has to be investigated. This would impact the electronic structure, the reactivity of the complexes, and in fine the catalytic ability.

#### 4. Catalytic application of phosphasalen ligands in (lactide) ring opening polymerization

Up to now, the only reported catalytic performances for phosphasalen complexes concern the ring opening polymerization (ROP), of lactide mostly. Polylactide (PLA) is a

biodegradable polymer which has found numerous applications for packaging<sup>[28]</sup> and bio-medical materials.<sup>[29]</sup> The lactide derives from lactic acid which is produced from high starch content plant and can therefore offer a sustainable alternative to petrochemicals. That is why there is a growing interest in the preparation of well-defined PLA, which is efficiently obtained by a controlled polymerization of lactide. This can be catalyzed by enzymes,<sup>[30]</sup> organic molecules,<sup>[31]</sup> and metal amide or alkoxide complexes,<sup>[32]</sup> for which a careful design of the ancillary ligand may lead to high stereoselectivities. Indeed, lactide has two chiral centers and can exist as three stereoisomers: the *D*-lactide (combining two *R*-lactic acids), the *L*-lactide (containing two *S*-lactic acids) and the *meso*-lactide (a combination of *R* and *S*-lactic acids, Scheme 4).



**Scheme 4.** *rac*-Lactide polymerization.

Initiators able to promote the stereoselective production PLA from *rac*-lactide are highly desirable. Most initiators yield atactic or heteroatactic-PLA (formed by the alternative incorporation of *R,R* and *S,S*-lactic acids) whereas isotactic PLA (resulting from the incorporation of the same enantiomer, either *R,R* or *S,S*) have superior thermal and mechanical properties.<sup>[33]</sup> Group 3, and in particular Y<sup>III</sup> based initiators, are efficient and can be stereoselective.<sup>[34]</sup>

This has stimulated the evaluation of yttrium phosphasalen complexes for lactide ROP. The [Y(Psalfen)(O<sup>*t*</sup>Bu)] complex described by Diaconescu and coworkers (Figure 9), catalyzes the ring opening polymerization of lactide; 74 % conversion is observed for *L*-lactide after 3 h (Table 2, entry 1) and 95 % for *rac*-lactide using 100 equivalents of monomer. Most interestingly, the catalytic ability can be switched off by oxidizing the ferrocene unit present in the ligand backbone;<sup>[35]</sup> [Y(Psalfen)(O<sup>*t*</sup>Bu)](BA<sup>F</sup><sub>4</sub>) was found unable to polymerize lactide. A stoichiometric experiment shows that the process stops with the insertion of one monomer molecule, because the propagation is hampered. In a reverse manner, they proved that trimethylcarbonate polymerization can be accelerated by oxidation in the case of an indium initiator ([In(Psalfen)(OPh)]).<sup>[35b]</sup>

Yttrium phosphasalen initiators were also developed for *rac*-LA polymerization. As coordination of the Psalen<sup>H</sup> ligand to Y<sup>III</sup> gave dimers (Figure 9), Psalen<sup>*t*Bu</sup> was used to avoid dimerization and improve solubility.<sup>[36]</sup> Complexes were obtained by coordination of the Psalen<sup>R</sup> ligands to [YCl<sub>3</sub>(THF)<sub>3.5</sub>] followed by metathesis of [Y(Psalen<sup>R</sup>)Cl] with R'<sup>+</sup>OK (R' = *t*Bu, Et), as depicted in Scheme 2. These complexes are rapid initiators for lactide polymerization and the process is well controlled (Table 4, entries 2-5). In particular, the performances of the monomeric [Y(Psalen<sup>*t*Bu</sup>)(O<sup>*t*</sup>Bu)] outstrip those of the dimers (Table 4, entries 2-4). This initiator is extremely active and shows a good control in presence of an exogenous alcohol as a chain transfer agent, as well as an excellent heteroselectivity at room temperature. It can be used at low loadings (down to 5000, see Table 4, entry 5), allowing the preparation of high molecular weight polylactide. Moreover, this initiator tolerates the use of unpurified lactide (Table 4, entry 6).<sup>[37]</sup>

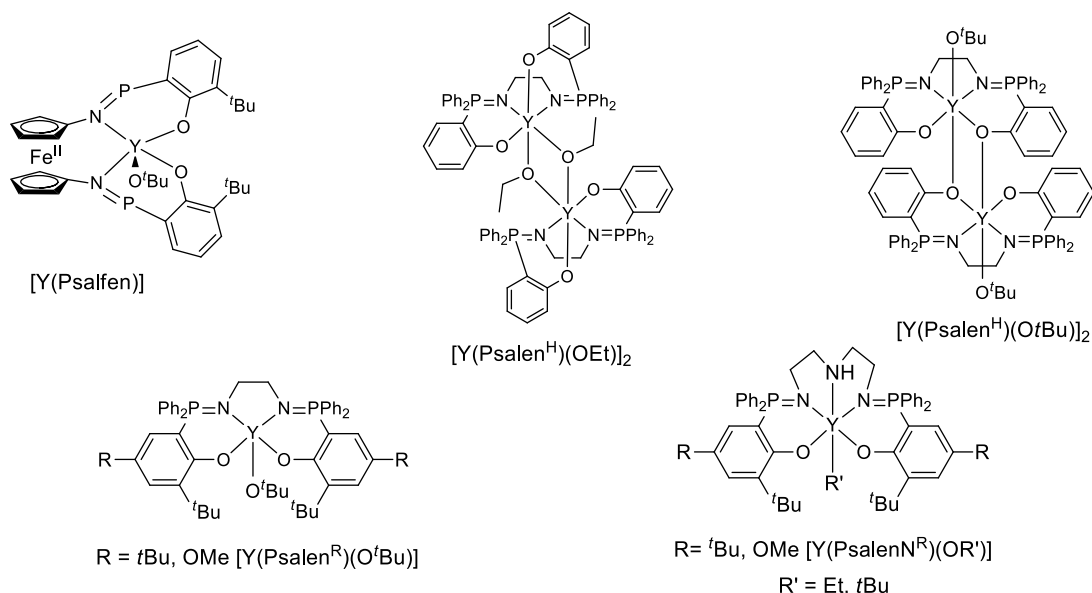


**Figure 9.** Yttrium phosphasalen initiators for lactide Ring Opening Polymerization.



**Table 3.** Data for the ROP of lactide with phosphasalén complexes in THF.

Entry	Initiator	[LA] <sub>0</sub> : [I](:[ <sup>i</sup> PrOH])	time	Conv. (%)	M <sub>n</sub> (kg mol <sup>-1</sup> )	M <sub>n</sub> <sup>calc</sup> (kg mol <sup>-1</sup> )	PDI	P <sub>s</sub>
1	[Y(Psalen)(O <i>t</i> Bu)] <sup>a</sup>	100:1	3 h	74	7.5	10.7	1.07	-
2	[Y(Psalen <sup>H</sup> )(OEt)] <sub>2</sub> <sup>b</sup>	200:1	56 min	90	27.1	25.9	1.36	0.78
3	[Y(Psalen <sup>H</sup> )(O <i>t</i> Bu)] <sub>2</sub> <sup>b</sup>	200:1	40 s	91	57.6	26.2	1.42	0.78
4	[Y(Psalen <sup>Et</sup> )(O <i>t</i> Bu)] <sup>b</sup>	1000:1:1	70 s	80	105	115	1.08	0.90
5	[Y(Psalen <sup>Et</sup> )(O <i>t</i> Bu)] <sup>b</sup>	5000:1	30 min	98	720	700	1.23	0.88
6	[Y(Psalen <sup>Et</sup> )(O <i>t</i> Bu)] <sup>b</sup>	1000:1 <sup>c</sup>	120 s	99	144	332	1.31	0.87
7	[Y(Psalen <sup>OMe</sup> )(O <i>t</i> Bu)] <sup>b</sup>	1000:1	20 s	88	165	128.7	1.50	0.87
8	[Y(PsalenN <sup>Et</sup> )(O <i>t</i> Bu)] <sup>b</sup>	500:1:1	56 min	92	41	66.2	1.05	0.26
9	[Y(PsalenN <sup>Et</sup> )(O <i>t</i> Bu)] <sup>b,d</sup>	100:1:1	3 h	77	16	11.1	1.01	0.16
10	[Y(PsalenN <sup>Et</sup> )(OEt)] <sup>b</sup>	500:1	48 min	85	61.7	61.2	1.04	0.28
11	[Y(PsalenN <sup>Et</sup> )(OEt)] <sup>b,d</sup>	500:1	3 h	73	13.5	10.5	1.01	0.19
12	[Y(PsalenN <sup>Et</sup> )(OEt)] <sup>b,d</sup>	500:1	30 min	85	48.6	61.2	1.08	0.22
13	[Lu(PsalenN <sup>Et</sup> )(OEt)] <sup>b</sup>	500:1	8.25 h	86	53.4	61.9	1.02	0.18
14	[La(PsalenN <sup>Et</sup> )(O <i>t</i> Bu)] <sup>b</sup>	500:1:1	20 s	98	57.3	70.6	1.05	0.72
15	[In(Psalen <sup>PhMe2</sup> )(OEt)] <sup>b</sup>	500:1	1 h	96	65.3	69.2	1.15	0.13

<sup>a</sup> [L-LA]<sub>0</sub> = 2 M, 298 K. <sup>b</sup> [rac-LA]<sub>0</sub> = 1 M, 298 K. <sup>c</sup> reaction using unpurified lactide. <sup>d</sup> at 258 K, [LA]<sub>0</sub> = 0.5 M.

The control of the molecular mass is not optimal with the *tert*-butoxide complex but it was improved by adding one equivalent of isopropanol as a chain transfer agent (see Table 4, entries 4, 8, and 9). Most importantly, these yttrium based catalysts are stereoselective, leading to heterotactic polylactide. The best stereoselectivity in this series was observed for [Y(Psalen<sup>Et</sup>)(O*t*Bu)] with P<sub>s</sub> around 0.9. These performances are much better than those of the salen analogues which present higher Lewis acidity.<sup>[38]</sup> This exceptional activity was ascribed to an easier migration of the alkoxide chain thanks to the higher electron-donating ability of the phosphasalén, which facilitates the propagation. This more than compensates the more difficult coordination of the monomer (due to the reduced Lewis acidity). Moreover, the flexibility of phosphasalén ligands may also be beneficial since the coordination sphere of the yttrium is expected to change much during the coordination-insertion steps in the ring opening polymerization.<sup>[36]</sup> In order to improve the catalytic performances, the structure of the phosphasalén ligand was modified. Psalen<sup>OMe</sup> was employed (Figure 9) to further increase the electron density at the metal. [Y(Psalen<sup>OMe</sup>)(O*t*Bu)], is a slightly more rapid initiator than [Y(Psalen<sup>Et</sup>)(O*t*Bu)] (Table 4, entries 4 and 7); the polymerization control was also improved by adding one equivalent of isopropanol. Importantly, the tacticity control remains excellent.<sup>[39]</sup> Other yttrium complexes differing by the nature of the nitrogen linker were synthesized. The rate of polymerization as well as the heterotactic bias decrease when replacing the ethylene linker by a cyclohexene, phenylene, or propylene one.<sup>[40]</sup> However, the use of a pentadentate ligand incorporating a supplementary coordinating amine led to a

powerful initiator.<sup>[39]</sup> Noteworthy, in [Y(PsalenN<sup>Et</sup>)(OR')] (R' = Et, *t*Bu) complexes (Figure 4), the yttrium has a different coordination environment since the phosphasalén adopts a *cis*-β configuration and not a *trans* one. These complexes were found very active in the lactide ROP, although less rapid than [Y(Psalen<sup>Et</sup>)(OR')] (Table 4, entries 4, 8, and 10).<sup>[39]</sup> Again, with a *tert*-butoxide initiator, the addition of an exogenous alcohol is necessary to ensure a good control of the polymerization (Table 4, entry 8 vs 10). The most striking point is the stereoselectivity, as [Y(PsalenN<sup>Et</sup>)(OR')] initiators yield isotactic polylactide with P<sub>i</sub> values of about 0.73 at 298 K to a maximum of 0.84 at 258 K (Table 4, entry 9).<sup>[39]</sup> This unexpected change of stereoselection by a simple modification of the ligand backbone was quite unprecedented and was explained by the more congested and constrained active site in hexacoordinated yttrium complexes. The modification of the ligand via the introduction of methoxy substituents allows an increased activity with a comparable isotacticity (Table 4, entries 10 and 12).<sup>[41]</sup>

In attempt to further improve the catalytic performances, the group of C. K. Williams employed other metals (Figure 10). With lutetium, a lanthanide with a slightly smaller covalent radius than yttrium (1.87 vs 1.90 Å), the isotacticity of the polymerization was improved to reach P<sub>i</sub> = 0.87 at room temperature (Table 4, entry 12) and 0.89 at 257 K.<sup>[42]</sup> This higher stereoselectivity was ascribed to a more constrained coordination sphere for the lutetium, which also induces a lower catalytic activity compared to yttrium (Table 4, entries 10 and 13).

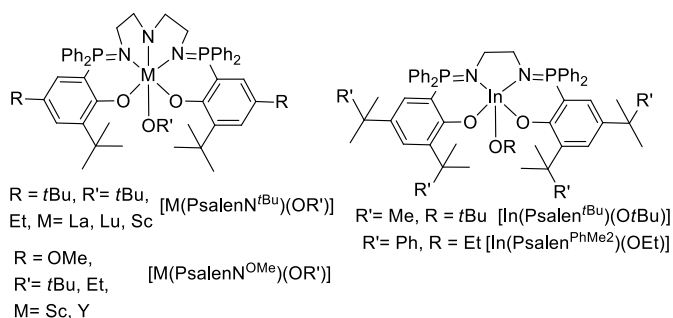


**Figure 10.** Other phosphasalen initiators for ROP.

Following this trend, no lactide polymerization was observed for the scandium based initiator ( $[Sc(PsalenN^{tBu})]$ ).<sup>[41]</sup> But this initiator allows a slow but controlled polymerization of  $\epsilon$ -caprolactone. Conversely, lanthanum initiator incorporating a larger metal (covalent radius of 2.07 Å) gave a very rapid polymerization, with a moderate heteroselectivity ( $P_s = 0.72$ , Table 4, entry 14).<sup>[42]</sup> NMR studies evidenced a more fluxional structure for La compared to Y and Lu complexes, suggesting that the stereocontrol depends on the level of the rigidity dictated by the ligand. Aiming at developing more rapid and isoselective lactide polymerization initiators, the Williams' group investigated the combination of phosphasalen ligand and  $In^{3+}$  cation.<sup>[43]</sup> As coordination experiments with the pentadentate  $PsalenN^{tBu}$  ligand gave a mixture of products, the study was conducted with two tetradentate ligands featuring an ethylene linker,  $Psalen^{tBu}$  and  $Psalen^{PhMe_2}$ , which differ from the precedent by the replacement of *tert*-butyl groups on the phenoxide by cumyl ones (Figure 10).<sup>[43]</sup> Solid state structures were different for both complexes as  $[In(Psalen^{tBu})(OtBu)]$  was characterized as a monomer, and  $[In(Psalen^{PhMe_2})(OEt)]$  as a dimer with bridging ethoxide. These differences were related to the size of the alkoxide ligand. Nevertheless, in a coordinating solvent such as THF, both complexes were found mononuclear, and the same is presumed during polymerization. The best isoselectivity was observed with  $[In(Psalen^{PhMe_2})(OEt)]$  (Table 4, entry 15), giving  $P_i = 0.92$  at 258 K. Interestingly, this catalyst allows a high degree of isoselectivity together with a rapid polymerization; it is as rapid as  $[Y(PsalenN^{tBu})(OtBu)]$  (Table 4, entries 8 and 15) and more selective than  $[Lu(PsalenN^{tBu})(OEt)]$  (Table 4, entries 13 and 15). Therefore, indium  $Psalen$  complexes show much higher polymerization rates than indium  $salen$  complexes with isoselectivity comparable to those of aluminium  $salen$  initiators.

These first catalytic studies evidenced that the performances of the phosphasalen complexes can be nicely tuned by modifying the phenoxide substituents, the N,N linker, as well as the metals. To date, no report deals with the influence of the phosphorous substituents on the catalytic ability. Moreover, considering the numerous applications of  $salen$  or  $salan$  ligands in catalysis, far beyond polymerization processes, this new family of ligands should find in the future other interesting applications.

## 5. Conclusion

Phosphasalens were first described six years ago and have since shown interesting properties. Importantly, they are relatively easy to synthesize; the Kirsanov method has the advantage to use commercial diamine but the Staudinger reaction is also a valuable option when the diazide is stable and easy to access. As expected, phosphasalens exhibit better donating abilities compared to  $salen$ . They also offer a larger coordination sphere (longer M-N and M-O bonds). The P=N bond, which is longer than the imine one, and the tetrahedral geometry of the phosphorus compared to the  $sp^2$  hybridization of the imine carbon in  $salen$ , play an essential role in the properties of phosphasalens. This leads to a more sterically hindered second coordination sphere and allow an increased flexibility compared to  $salen$ . The investigation of the one-electron oxidation of phosphasalen complexes showed that this ligand favors a metal-centered oxidation, allowing the stabilization of nickel(III) and copper(III) centers in a square planar environment. Thus, phosphasalen is a valuable alternative to  $salen$  when seeking to stabilize electron deficiency on the metal center. Moreover, the oxidation locus can be finely tuned by modifying the ligand structure of  $Psalen$  as exemplified with the introduction of methoxy groups. Both electronic and geometric considerations can explain the higher ligand radical character of the  $Psalen^{OMe}$  mono-oxidized complexes. Most importantly, the contradictory experimental results as well as theoretical investigations point towards a multi-configurational ground state for these complexes. This is another contribution to the literature concerning the difficult description of the spectroscopic oxidation state in presence of redox non-innocent ligands. The peculiar coordination environment created by the phosphasalen platform was also exploited in catalysis for the ring opening polymerization, of lactide mainly. It was demonstrated that the reduced Lewis acidity of those complexes did not hamper their reactivity since it is compensated by an easier migration of the alkoxide, allowing a rapid propagation. Yttrium, lutetium and indium phosphasalen complexes are outstanding catalysts for the ROP of lactide exhibiting a high activity, a good control of the molecular mass, as well as a high stereoselectivity. Heteroselective and isoselective catalysts were described. The switch in the stereochemical outcome of the reaction was, in some cases, done by modifying the N,N linker in the ligand backbone. These studies are very promising concerning the potential of phosphasalen complexes in catalysis, especially for reactions involving the transfer of a nucleophile from the metal to the substrate. As its carbon analogue  $salen$ , has been established over the years as a powerful ligand in catalysis and especially in asymmetric catalysis, developments of phosphasalen complexes in this area are expected in the future.

## Acknowledgements

A.A. thank T.-P.-A. Cao, who initiated the chemistry of phosphasalens ligands and persevered despite the initial synthetic difficulties. CNRS and Ecole polytechnique are

acknowledged for their financial support as well as the ANR which funded the PsalenOx project regarding the oxidation of phosphasalen complexes (JCC project n°13-JS07-0001-01).

**Keywords:** salen type ligands • redox non-innocent ligand • phosphorus oxidation • catalysis

- [1] S. Bellemin-Laponnaz, S. Dagorne, *Coordination Chemistry and Applications of Salen, Salan and Salalen Metal Complexes*, in PATAI'S Chemistry of Functional Groups, John Wiley & Sons, Ltd, **2012**.
- [2] a) P. G. Cozzi, *Chem. Soc. Rev.* **2004**, *33*, 410-421; b) N. S. Venkataramanan, G. Kuppuraj, S. Rajagopal, *Coord. Chem. Rev.* **2005**, *249*, 1249-1268; c) C. Baleizao, H. Garcia, *Chem. Rev.* **2006**, *106*, 3987-4043; d) D. J. Darensbourg, *Chem. Rev.* **2007**, *107*, 2388-2410; e) R. M. Haak, S. J. Wezenberg, A. W. Kleij, *Chem. Commun.* **2010**, *46*, 2713-2723; f) A. Zulauf, M. Mellah, X. A. Hong, E. Schulz, *Dalton Trans.* **2010**, *39*, 6911-6935.
- [3] a) C. T. Lyons, T. D. P. Stack, *Coord. Chem. Rev.* **2013**, *257*, 528-540; b) R. M. Clarke, T. Storr, *Dalton Trans.* **2014**, *43*, 9380-9391; c) J. Ciccione, N. Leconte, D. Luneau, C. Philouze, F. Thomas, *Inorg. Chem.* **2016**, *55*, 649-665; d) H.-Y. Yin, J. Tang, J.-L. Zhang, *Eur. J. Inorg. Chem.* **2017**, 5085-5093.
- [4] a) S. J. Wezenberg, A. W. Kleij, *Angew. Chem. Int. Ed.* **2008**, *47*, 2354-2364; b) J. Chun, S. Kang, N. Kang, S. M. Lee, H. J. Kim, S. U. Son, *J. Mater. Chem. A* **2013**, *1*, 5517-5523; c) L. H. Li, X. L. Feng, X. H. Cui, Y. X. Ma, S. Y. Ding, W. Wang, *J. Am. Chem. Soc.* **2017**, *139*, 6042-6045.
- [5] a) S. Halder, R. Acharyya, S.-M. Peng, G.-H. Lee, M. G. B. Drew, S. Bhattacharya, *Inorg. Chem.* **2006**, *45*, 9654-9663; b) S. B. Choudhury, D. Ray, A. Chakravorty, *J. Chem. Soc. Dalton Trans.* **1992**, 107-112.
- [6] E. M. Broderick, P. S. Thuy-Boun, N. Guo, C. S. Vogel, J. T. Miller, K. Meyer, P. L. Diaconescu, *Inorg. Chem.* **2011**, *50*, 2870-2877.
- [7] T. P. A. Cao, S. Labouille, A. Auffrant, Y. Jean, X. F. Le Goff, P. Le Floch, *Dalton Trans.* **2011**, *40*, 10029-10037.
- [8] a) T. P. A. Cao, Coordination chemistry and catalysis with mixed ligands associating iminophosphorane to thiolate or phenolate, PhD thesis, Ecole Polytechnique (Palaiseau), **Septembre 2012**; b) A. Buchard, Chimie de coordination des iminophosphoranes et nouveaux systèmes catalytiques, PhD thesis, Ecole Polytechnique (Palaiseau), **Septembre 2009**.
- [9] H. Staudinger, J. Meyer, *Helv. Chim. Acta* **1919**, 635.
- [10] a) L. Horner, H. Oediger, *Justus Liebig An. Chem.* **1959**, *627*, 142-162; b) I. N. Zhmurova, A. V. Kirsanov, *J. Gen. Chem. USSR* **1961**, *31*, 3440-8; c) I. N. Zhmurova, A. V. Kirsanov, *J. Gen. Chem. USSR* **1962**, *32*, 2540-8; d) I. N. Zhmurova, A. V. Kirsanov, *J. Gen. Chem. USSR* **1963**, *33*, 1004-8; e) H. Zimmer, G. Singh, *J. Org. Chem.* **1963**, *28*, 483-8.
- [11] a) M. Kondo, K. Nabari, T. Horiba, Y. Irie, M. K. Kabir, R. P. Sarker, E. Shimizu, Y. Shimizu, Y. Fuwa, *Inorg. Chem. Commun.* **2003**, *6*, 154-156; b) N. Kumari, R. Prajapati, L. Mishra, *Polyhedron* **2008**, *27*, 241-248.
- [12] a) I. C. Santos, M. Vilas-Boas, M. F. M. Piedade, C. Freire, M. T. Duarte, B. de Castro, *Polyhedron* **2000**, *19*, 655-664; b) S. V. Vasileva, K. P. Balashev, A. M. Timonov, *Russ. J. Electrochem.* **2000**, *36*, 75-79; c) J. Fonseca, J. Tedim, K. Biernacki, A. L. Magalhaes, S. J. Gurman, C. Freire, A. R. Hillman, *Electrochim. Acta* **2010**, *55*, 7726-7736.
- [13] a) R. C. Pratt, C. T. Lyons, E. C. Wasinger, T. D. P. Stack, *J. Am. Chem. Soc.* **2012**, *134*, 7367-7377; b) M. Orio, O. Jarjayes, H. Kanso, C. Philouze, F. Neese, F. Thomas, *Angew. Chem. Int. Ed.* **2010**, *49*, 4989-4992; c) T. Storr, P. Verma, R. C. Pratt, E. C. Wasinger, Y. Shimazaki, T. D. P. Stack, *J. Am. Chem. Soc.* **2008**, *130*, 15448-15459; d) Y. D. Wang, J. L. DuBois, B. Hedman, K. O. Hodgson, T. D. P. Stack, *Science* **1998**, *279*, 537-540; e) P. Chaudhuri, M. Hess, U. Florke, K. Wiegardt, *Angew. Chem. Int. Ed.* **1998**, *37*, 2217-2220; f) L. Chiang, K. Herasymchuk, F. Thomas, T. Storr, *Inorg. Chem.* **2015**, *54*, 5970-5980.
- [14] D. Tietze, H. Breitzke, D. Imhof, E. Kothe, J. Weston, G. Buntkowsky, *Chem. Eur. J.* **2009**, *15*, 517-523.
- [15] a) O. Rotthaus, O. Jarjayes, C. Philouze, C. P. Del Valle, F. Thomas, *Dalton Trans.* **2009**, 1792-1800; b) O. Rotthaus, O. Jarjayes, C. P. Del Valle, C. Philouze, F. Thomas, *Chem. Commun.* **2007**, 4462-4464; c) O. Rotthaus, F. Thomas, O. Jarjayes, C. Philouze, E. Saint-Aman, J. L. Pierre, *Chem.-Eur. J.* **2006**, *12*, 6953-6962; d) O. Rotthaus, O. Jarjayes, F. Thomas, C. Philouze, C. Perez Del Valle, E. Saint-Aman, J.-L. Pierre, *Chem. Eur. J.* **2006**, *12*, 2293-2302; e) B. Decastro, C. Freire, *Inorg. Chem.* **1990**, *29*, 5113-5119.
- [16] a) F. Thomas, *Dalton Trans.* **2016**, *45*, 10866-10877; b) L. Chiang, A. Kochem, O. Jarjayes, T. J. Dunn, H. Vezin, M. Sakaguchi, T. Ogura, M. Orio, Y. Shimazaki, F. Thomas, T. Storr, *Chem.-Eur. J.* **2012**, *18*, 14117-14127; c) T. Kurahashi, H. Fujii, *J. Am. Chem. Soc.* **2011**, *133*, 8307-8316; d) Y. Shimazaki, T. D. P. Stack, T. Storr, *Inorg. Chem.* **2009**, *48*, 8383-8392; e) Y. Shimazaki, T. Yajima, F. Tani, S. Karasawa, K. Fukui, Y. Naruta, O. Yamauchi, *J. Am. Chem. Soc.* **2007**, *129*, 2559-2568.
- [17] a) S. F. Hannigan, J. S. Lum, J. W. Bacon, C. Moore, J. A. Golen, A. L. Rheingold, L. H. Doerrer, *Organometallics* **2013**, *32*, 3429-3436; b) C. J. Cramer, W. B. Tolman, *Acc. Chem. Res.* **2007**, *40*, 601-608; c) J. L. DuBois, P. Mukherjee, T. D. P. Stack, B. Hedman, E. I. Solomon, K. O. Hodgson, *J. Am. Chem. Soc.* **2000**, *122*, 5775-5787.
- [18] a) M. B. Watson, N. P. Rath, L. M. Mirica, *J. Am. Chem. Soc.* **2017**, *139*, 35-38; b) E. Chong, J. W. Kampf, A. Ariafard, A. J. Canty, M. S. Sanford, *J. Am. Chem. Soc.* **2017**, *139*, 6058-6061; c) G. E. Martinez, C. Ocampo, Y. J. Park, A. R. Fout, *J. Am. Chem. Soc.* **2016**, *138*, 4290-4293.
- [19] J. R. Bour, N. M. Camasso, M. S. Sanford, *J. Am. Chem. Soc.* **2015**, *137*, 8034-8037.
- [20] a) J. C. Tellis, C. B. Kelly, D. N. Primer, M. Jouffroy, N. R. Patel, G. A. Molander, *Acc. Chem. Res.* **2016**, *49*, 1429-1439; b) J. R. Bour, N. M. Camasso, E. A. Meucci, J. W. Kampf, A. J. Canty, M. S. Sanford, *J. Am. Chem. Soc.* **2016**, *138*, 16105-16111.
- [21] a) A. Casitas, X. Ribas, *Chem. Sci.* **2013**, *4*, 2301-2318; b) M. Rovira, M. Font, F. Acuna-Pares, T. Parella, J. M. Luis, J. Lloret-Fillol, X. Ribas, *Chem.-Eur. J.* **2014**, *20*, 10005-10010; c) D. Holt, M. J. Gaunt, *Angew. Chem. Int. Ed.* **2015**, *54*, 7857-7861; d) J. C. Vantourout, H. N. Miras, A. Isidro-Llobet, S. Sproules, A. J. B. Watson, *J. Am. Chem. Soc.* **2017**, *139*, 4769-4779; e) A. D. Spaeth, N. L. Gagnon, D. Dhar, G. M. Yee, W. B. Tolman, *J. Am. Chem. Soc.* **2017**, *139*, 4477-4485.
- [22] a) C. M. Lemon, M. Huynh, A. G. Maher, B. L. Anderson, E. D. Bloch, D. C. Powers, D. G. Nocera, *Angew. Chem. Int. Ed.* **2016**, *55*, 2176-2180; b) J. Zapata-Rivera, R. Caballol, C. J. Calzado, *J. Comput. Chem.* **2011**, *32*, 1144-1158; c) J. Zapata-Rivera, R. Caballol, C. J. Calzado, *Phys. Chem. Chem. Phys.* **2011**, *13*, 20241-20247; d) N. C. Tomson, M. R. Crimmin, T. Petrenko, L. E. Rosebrugh, S. Sproules, W. C. Boyd, R. G. Bergman, S. DeBeer, F. D. Toste, K. Wiegardt, *J. Am. Chem. Soc.* **2011**, *133*, 18785-18801; e) C. E. Ruggiero, S. M. Carrier, W. E. Antholine, J. W. Whittaker, C. J. Cramer, W. B. Tolman, *J. Am. Chem. Soc.* **1993**, *115*, 11285-11298; f) S. M. Carrier, C. E. Ruggiero, W. B. Tolman, G. B. Jameson, *J. Am. Chem. Soc.* **1992**, *114*, 4407-4408.
- [23] T. P. A. Cao, G. Nocton, L. Ricard, X. F. Le Goff, A. Auffrant, *Angew. Chem. Int. Ed.* **2014**, *53*, 1368-1372.
- [24] I. Mustieles-Marín, T. Cheisson, R. Singh Chauhan, C. Herrero, M. Cordier, C. Clavaguéra, G. Nocton, A. Auffrant, *Chem. Eur. J.*, *10.1002/chem.201703390*.
- [25] L. Benisvy, R. Kannappan, Y. F. Song, S. Miliukisants, M. Huber, I. Mutikainen, U. Turpeinen, P. Gamez, L. Bernasconi, E. J. Baerends, F. Hartl, J. Reedijk, *Eur. J. Inorg. Chem.* **2007**, 637-642.
- [26] F. Thomas, O. Jarjayes, C. Duboc, C. Philouze, E. Saint-Aman, J. L. Pierre, *Dalton Trans.* **2004**, 2662-2669.

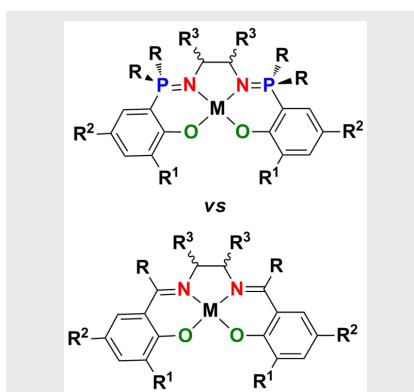
- 
- [27] a) C. H. Booth, D. Kazhdan, E. L. Werkema, M. D. Walter, W. W. Lukens, E. D. Bauer, Y. J. Hu, L. Maron, O. Eisenstein, M. Head-Gordon, R. A. Andersen, *J. Am. Chem. Soc.* **2010**, *132*, 17537-17549; b) C. H. Booth, M. D. Walter, D. Kazhdan, Y. J. Hu, W. W. Lukens, E. D. Bauer, L. Maron, O. Eisenstein, R. A. Andersen, *J. Am. Chem. Soc.* **2009**, *131*, 6480-6491.
- [28] M. Jamshidian, E. A. Tehrani, M. Imran, M. Jacquot, S. Desobry, *Compr. Rev. Food. Sci. Food Saf.* **2010**, *9*, 552-571.
- [29] a) B. D. Ulery, L. S. Nair, C. T. Laurencin, *J. Polym. Sci. Pt. B-Polym. Phys.* **2011**, *49*, 832-864; b) K. E. Uhrich, S. M. Cannizzaro, R. S. Langer, K. M. Shakesheff, *Chem. Rev.* **1999**, *99*, 3181-3198.
- [30] a) H. O. Duskunkorur, A. Begue, E. Pollet, V. Phalip, Y. Guvenilir, L. Averous, *J. Mol. Catal. B-Enzym.* **2015**, *115*, 20-28; b) S. W. Duchiron, E. Pollet, S. Givryb, L. Averous, *RSC Adv.* **2015**, *5*, 84627-84635; c) R. A. Gross, A. Kumar, B. Kalra, *Chem. Rev.* **2001**, *101*, 2097-2124.
- [31] N. E. Kamber, W. Jeong, R. M. Waymouth, R. C. Pratt, B. G. G. Lohmeijer, J. L. Hedrick, *Chem. Rev.* **2007**, *107*, 5813-5840.
- [32] a) A. Sauer, A. Kapelski, C. Fliedel, S. Dagorne, M. Kol, J. Okuda, *Dalton Trans.* **2013**, *42*, 9007-9023; b) N. Ajellal, J. F. Carpentier, C. Guillaume, S. M. Guillaume, M. Helou, V. Poirier, Y. Sarazin, A. Trifonov, *Dalton Trans.* **2010**, *39*, 8363-8376.
- [33] a) M. Kakuta, M. Hirata, Y. Kimura, *Polym. Rev.* **2009**, *49*, 107-140; b) Y. Ikada, K. Jamshidi, H. Tsuji, S. H. Hyon, *Macromolecules* **1987**, *20*, 904-906.
- [34] a) X. L. Liu, X. M. Shang, T. Tang, N. H. Hu, F. K. Pei, D. M. Cui, X. S. Chen, X. B. Jing, *Organometallics* **2007**, *26*, 2747-2757; b) E. Grunova, E. Kirillov, T. Roisnel, J. F. Carpentier, *Organometallics* **2008**, *27*, 5691-5698; c) P. L. Arnold, J. C. Buffet, R. P. Blaudeck, S. Sujecki, A. J. Blake, C. Wilson, *Angew. Chem. Int. Ed.* **2008**, *47*, 6033-6036; d) R. H. Platel, A. J. P. White, C. K. Williams, *Chem. Commun.* **2009**, 4115-4117.
- [35] a) E. M. Broderick, N. Guo, T. P. Wu, C. S. Vogel, C. L. Xu, J. Sutter, J. T. Miller, K. Meyer, T. Cantat, P. L. Diaconescu, *Chem. Commun.* **2011**, *47*, 9897-9899; b) E. M. Broderick, N. Guo, C. S. Vogel, C. Xu, J. Sutter, J. T. Miller, K. Meyer, P. Mehrkhodavandi, P. L. Diaconescu, *J. Am. Chem. Soc.* **2011**, *133*, 9278-9281.
- [36] T. P. A. Cao, A. Buchard, X. F. Le Goff, A. Auffrant, C. K. Williams, *Inorg. Chem.* **2012**, *51*, 2157-2169.
- [37] Usually lactide used for ROP is sublimed and recrystallized several times to ensure a high level of purity. Impurities present are among other water and lactic acid. Lactide obtained from chemical supplier is indicated as 98% or 99% pure.
- [38] a) A. Alaaeddine, C. M. Thomas, T. Roisnel, J.-F. Carpentier, *Organometallics* **2009**, *28*, 1469-1475; b) T. M. Ovitt, G. W. Coates, *J. Am. Chem. Soc.* **2002**, *124*, 1316-1326.
- [39] C. Bakewell, T. P. A. Cao, N. Long, X. F. Le Goff, A. Auffrant, C. K. Williams, *J. Am. Chem. Soc.* **2012**, *134*, 20577-20580.
- [40] C. Bakewell, T. P. A. Cao, X. F. Le Goff, N. J. Long, A. Auffrant, C. K. Williams, *Organometallics* **2013**, *32*, 1475-1483.
- [41] C. Bakewell, A. J. P. White, N. J. Long, C. K. Williams, *Inorg. Chem.* **2015**, *54*, 2204-2212.
- [42] C. Bakewell, A. J. P. White, N. J. Long, C. K. Williams, *Angew. Chem. Int. Ed.* **2014**, *53*, 9226-9230.
- [43] D. Myers, A. J. P. White, C. M. Forsyth, M. Bown, C. K. Williams, *Angew. Chem. Int. Ed.* **2017**, *56*, 5277-5282.
-

---

## MICROREVIEW

---

Phosphasalen complexes featuring a tetradentate  $N_2O_2$  ligand can be viewed as the phosphorous analogues of salen in which iminophosphoranes (P=N) replace imines. The presence of the phosphorus influences both the electronic properties and the steric hindrance. This was demonstrated by studies regarding the electronic structure of one-electron oxidized complexes as well as the catalytic abilities of phosphasalen complexes in ROP reactions.



*Phosphasalen complexes Author(s),*

*Irene Mustieles Marín, and Audrey*

*Aufrant\**

**Page No. – Page No.**

**Phosphasalen vs salen ligands: what does the phosphorus change?**

---